Support information for

Impact of metal cations on the electrocatalytic properties of Pt/C nanoparticles at multiple phase interfaces

By Julien Durst, Marian Chatenet and Frédéric Maillard

I. Cobalt doping of the Nafion® 117 membranes

After contamination with Co^{2+}-containing solutions, the extent of pollution of the Nafion® 117 membranes ($\gamma_{Co^{2+},membrane}$) is quantified by X-ray energy-dispersive spectroscopy (X-EDS). The amount of contamination of the liquid and solid electrolytes is expressed with the following relation:

$$\gamma_{Co^{2+}} = \frac{c_{Co^{2+}}}{c_{H^+} + c_{Co^{2+}}} \qquad\qquad (Eq. 1)$$

Figure S1 shows the membrane cationic composition ($\gamma_{Co2+, membrane}$) at equilibrium versus solution composition ($\gamma_{Co2+, solution}$) for Nafion® 117 PEMs. The plot translates the higher affinity of the sulfonate groups of the Nafion® membrane for Co^{2+} ions than for protons (at a given Co^{2+} concentration in solution, $\gamma_{Co^{2+},membrane} > \gamma_{Co^{2+},solution}$). The trend of this curve is in agreement with the data reported by Okada *et al.* [7] for other +II charged species (Fe^{2+}, Ni^{2+}, Cu^{2+}).
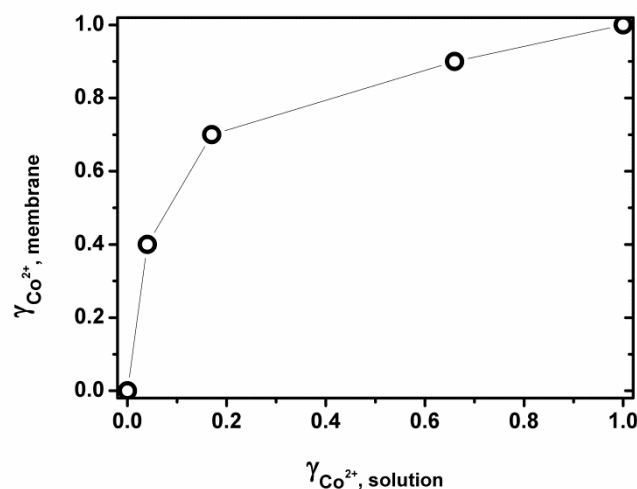

Figure S1 Membrane cationic composition (γ_{Co}^{2+}, membrane) at equilibrium versus solution composition (γ_{Co}^{2+}, solution) for Nafion® 117 PEMs at room temperature.

II. Calculation of D_{O_2}, C_{O_2} and v values in various electrolyte concentrations

The presence of solvated metal cations in liquid/solid electrolyte induces a decrease of the ORR diffusion limited current, j_D, which is given by the Levich equation:

$$j_D = 0.62 n F D_{O_2}^{2/3} C_{O_2} v^{-1/6} \omega^{1/2} \qquad\qquad (Eq. 2)$$

Rotating ring disk electrode (RRDE) measurements show that the number of exchanged electrons per O_2 molecule (see n in Table S1) decreases in the presence of solvated metal cations. However, the observed decreased of n cannot account for the changes of j_D (Table S1). This result suggests that the O_2 transport properties, namely the oxygen diffusion coefficient D_{O_2},

the kinematic viscosity v and the oxygen solubility C_{O_2}, are greatly affected by the presence of solvated metal cations in the electrolyte. In this section, these parameters are measured in oxygen-saturated 0.1 M H_2SO_4 and in 0.1 M H_2SO_4 + 0.1 M $CoSO_4$ solutions.

The oxygen diffusion coefficient D_{O_2} is determined from Cottrell-like chronoamperometry experiments, performed on an ultramicroelectrode with cavity (UMEC) filled with a Pt/C powder (30 wt. %, E-TEK). In this technique, first published by Denuault et al.[1] for a gold microdisk and later on optimized by Wang et al.[2] for a gold microsphere, the ultramicroelectrode is polarized at a potential where the ORR does not occur (here $U = 1.1$ V vs. RHE for $t = 30$ s) and then in a potential region where the oxygen reduction is diffusion limited (here $U = 0.4$ V *vs.* RHE for $t = 10$ s). The current transient during the potential step is recorded every $t = 10$ ms. From the slope S and the intercept A of the $I = f(t^{-1/2})$ plot (Figure S2), the oxygen diffusion coefficient can be determined using Eq. 3 (see Table S1):

$$D_{O_2} = \frac{r^2 \times A^2}{\pi \times S^2}$$
(Eq. 3)

with r the radius of the ultramicroelectrode ($r = 17$ μm). The oxygen coefficient calculated in 0.1 M H_2SO_4, $D_{O_2} = 1.9 \times 10^{-5}$ cm^2 s^{-1}, compares well with the value determined by Dubau et al. [3] in the same electrolyte. In the presence of Co^{2+} ions in solution, the oxygen diffusion coefficient is decreased by *ca.* 16 % to $D_{O_2} = 1.6 \times 10^{-5}$ cm^2 s^{-1}.
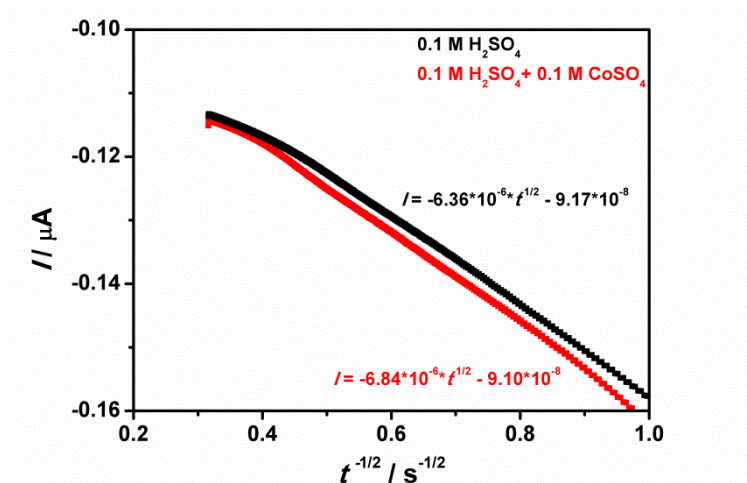

Figure S2 Cottrell lines relative to a potential step from $U = 1.1$ V *vs.* RHE to $U = 0.4$ V *vs.* RHE in oxygen saturated 0.1 M H_2SO_4 (black square symbols) and in in oxygen saturated 0.1 M H_2SO_4 + 0.1 M $CoSO_4$ (red square symbols). Sampling time = 10 ms. The linear regression of the corresponding curves are displayed in the graph.

With the calculated values of the oxygen diffusion coefficient, the kinematic viscosity of both solutions is determined with the oxygen diffusivity transient method on a rotating ring disk electrode. This method was first introduced by Gan and Chin[4] and Lozar et al.[5] according to the Bruckenstein and Feldman equation. [6] Practically speaking, a potential step (from $U_{disk} = 1.1$ V *vs.* RHE to $U_{disk} = 0.4$ V *vs.* RHE) is applied on the disk while in the same time the ring potential is maintained at a potential where oxygen is reduced ($U_{ring} = 0.4$ V *vs.* RHE). During the potential step of the disk, a depletion of oxygen is created and reaches the vicinity of the ring after a transit time t_s (s). This time t_s can be expressed as follow (Eq. 4):

$$t_s = K \times \left(\frac{v}{D_{O_2}}\right)^{1/3} \times \Omega^{-1}$$
(Eq. 4)

where Ω is the electrode rotation speed (in rpm) and K a coefficient characteristic of the geometry of the RRDE. For an ideal RRDE, it can be calculated with Eq. 5:

$$K = 43.1 \times \left(\log[\frac{r_2}{r_1}]\right)^{2/3}$$
(Eq. 5)

Where r_2 is the inside radius of the ring electrode (in cm) and r_1 the radius of the disk electrode (in cm). Here, we emphasize that for these calculations, we used the same set-up as in the experimental section of the paper ($K = 7.94$ rpm).

Therefore, from the slope of the $I = f(t^{-1/2})$ graph (Figure S3), the kinematic viscosities in both electrolytes can be calculated. Similar as for the oxygen diffusion coefficient, the presence of solvated cations such as Co^{2+} induces non-negligible decrease of the kinematic viscosity (Table S1). Finally, with the measured value of j_D, n, D_{O_2} and v in each electrolytic solution, the oxygen solubility C_{O_2} in the presence/absence of solvated cobalt cations can be calculated with the Levich equation (see Eq. 2 in the paper) and is reported in Table S1. Similar to the observed trend for the oxygen diffusion coefficient, the values of the oxygen solubility decreases in Co^{2+}-containing electrolyte.
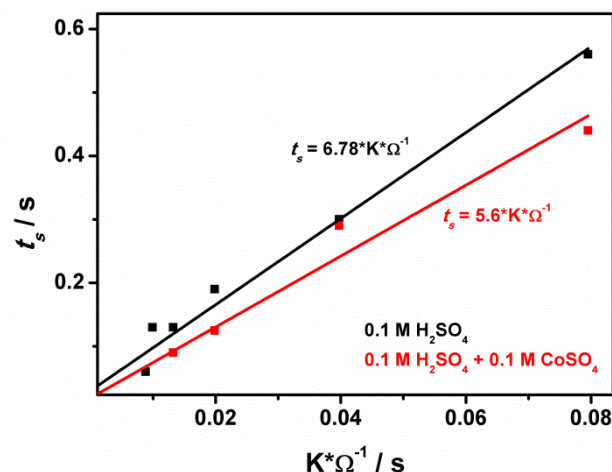

Figure S3 Transit time versus $K*\Omega^{-1}$ recorded in oxygen saturated 0.1 M H_2SO_4 (black square symbols) and 0.1 M H_2SO_4 + 0.1 M $CoSO_4$ (red square symbols). The results of the linear regressions of the data are displayed in the graph.

Table S1 ORR limiting current densities j_D (from Table 1), number of exchanged electrons n (from Table 1), kinematic viscosities v, oxygen diffusion coefficients D_{O_2} and solubilities C_{O_2} in 0.1 M H_2SO_4 in the presence/absence of 0.1 M $CoSO_4$.

	j_D / mA cm$_{geo}^{-2}$	n	D_{O_2} / cm^2 s^{-1}	v / cm^2 s^{-1}	C_{O_2} / mol cm^{-3}
0.1 M H_2SO_4	4.14	3.94	1.9×10^{-5}	0.60×10^{-2}	2.3×10^{-6}
0.1 M H_2SO_4 + 0.1 M Co^{2+} ($\gamma_{Co2+} = 0.66$)	3.42	3.88	1.6×10^{-5}	0.30×10^{-2}	1.9×10^{-6}

III. Cyclic voltammetry and CO stripping voltammograms in the solid state cell (SSC)

Figure S4 displays the cyclic voltammograms (CV) and the CO monolayer oxidation voltammograms recorded in the SSC with either a non-contaminated ($\gamma_{Co^{2+}} = 0$) or a contaminated ($\gamma_{Co^{2+}} = 0.9$) Nafion® 117 membrane. The CV (Figure S4.a) is greatly affected by the presence of Co^{2+} ions bounded to the sulfonate groups of the PEM: (i) the charge associated to the H_{upd} process increases and (ii) the formation of surface (hydr)oxides is favoured on Pt when Co^{2+} ions are present in the PEM, which suggests that Co^{2+} ions facilitate the oxidation of the Pt/C surface. Enhanced CO monolayer oxidation kinetics in the presence of Co^{2+} ions (Figure S4.b) suggests that Co^{2+} ions facilitate the formation of surface oxides on the Pt/C surface.
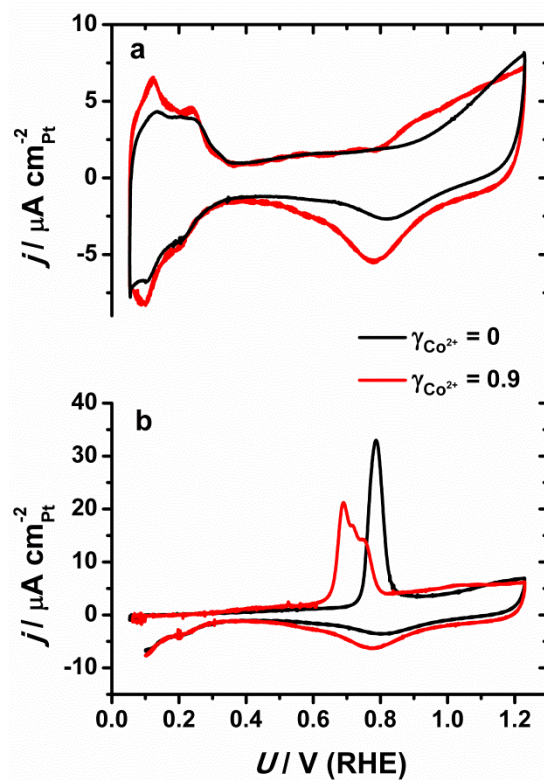
Figure S4 Base (a) and CO_{ad} stripping voltammograms (b) for Pt/C in contact with a non-contaminated ($\gamma_{Co^{2+}} = 0$) and a Co^{2+}-contaminated Nafion® 117 membrane ($\gamma_{Co^{2+}} = 0.9$). Temperature = 22 ± 1°C, Sweep rate = 0.005 V s^{-1}.

References

1. G. Denuault, M. V. Mirkin and A. J. Bard, *J. Electroanal. Chem.*, 1991, **308**, 27-38.
2. K. L. Wang, J. T. Lu and L. Zhuang, *J. Electroanal. Chem.*, 2005, **585**, 191-196.
3. L. Dubau, F. Maillard, M. Chatenet, J. Andre and E. Rossinot, *Electrochim. Acta*, 2010, **56**, 776-783.
4. F. Gan and D. T. Chin, *J. Appl. Electrochem.*, 1993, **23**, 452-455.
5. J. Lozar, B. Bachelot, G. Falgayrac and A. Savall, *Electrochim. Acta*, 1998, **43**, 3293-3296.
6. S. Bruckenstein and G. A. Feldman, *J. Electroanal. Chem.*, 1965, **9**, 395.
7. T. Okada, Y. Ayato, M. Yuasa and I. Sekine, *J. Phys. Chem. B*, 1999, **103**, 3315-3322.